

Comparison of results from a 2+1D relativistic viscous hydrodynamic model to elliptic and hexadecapole flow of charged hadrons measured in Au-Au collisions at $\sqrt{s_{NN}} = 200$ GeV

Victor Roy¹, A.K. Chaudhuri¹, and Bedangadas Mohanty^{1,2}

¹*Variable Energy Cyclotron Centre,
Kolkata 700064, India.*

and

²*School of Physical Sciences,
National Institute of Science Education and Research,
Bhubaneswar 751005, India.*

(Dated: November 11, 2018)

Simulated results from a 2+1D relativistic viscous hydrodynamic model have been compared to the experimental data on the centrality dependence of invariant yield, elliptic flow (v_2), and hexadecapole flow (v_4) as a function of transverse momentum (p_T) of charged hadrons in Au-Au collisions at $\sqrt{s_{NN}} = 200$ GeV. Results from two types of initial transverse energy density profile, one based on the Glauber model and other based on Color-Glass-Condensate (CGC) are presented. We observe no difference in the simulated results on the invariant yield of charged hadrons for the calculations with different initial conditions. The comparison to the experimental data on invariant yield of charged hadrons supports a shear viscosity to entropy density ratio (η/s) between 0 to 0.12 for the 0-10% to 40-50% collision centralities. The simulated $v_2(p_T)$ is found to be higher for a fluid with CGC based initial condition compared to Glauber based initial condition for a given collision centrality. Consequently the Glauber based calculations when compared to the experimental data requires a lower value of η/s relative to CGC based calculations. In addition, a centrality dependence of the estimated η/s is observed from the $v_2(p_T)$ study. The $v_4(p_T)$ for the collision centralities 0-10% to 40-50% supports a η/s value between 0 - 0.08 for a CGC based initial condition. While simulated results using the Glauber based initial condition for the ideal fluid evolution under estimates the $v_4(p_T)$ for collision centralities 0-10% to 30-40%.

PACS numbers: 25.75.Ld

I. INTRODUCTION

Heavy-ion collisions at the Relativistic Heavy Ion Collider (RHIC) have provided evidence for the formation of a hot and dense QCD matter [1–5]. This presents an unique opportunity to study the transport properties, like shear viscosity to entropy density ratio (η/s), of the QCD matter. There are two main theoretical approaches to estimate the value of η/s from the experimental data. One based on a microscopic approach as in transport theory [6–10] and other related to a macroscopic approach through relativistic viscous hydrodynamic calculations [11–18]. In this work, we will compare our results from a relativistic 2+1 dimension viscous hydrodynamics to recent high statistics experimental data on elliptic (v_2) and hexadecapole (v_4) flow of charged hadrons measured by the PHENIX Collaboration [19, 20]. The experimental observables related to azimuthal anisotropic flow are found to be sensitive to shear viscous effects. The shear viscosity decreases the anisotropy of the fluid velocity. Hence v_2 and v_4 as a function of transverse momentum (p_T) are expected to decrease with the increase in the value of η/s .

One of the main uncertainties in the estimation of η/s using a viscous hydrodynamics simulation is due

to the choice of the initial conditions [14, 17, 21]. In this work we have considered two models, Glauber and Color Glass Condensate (CGC), to obtain the initial transverse energy density profile. For this study we have considered a smooth initial condition, which does not vary event-by-event. Previous work have shown that both the spatial and momentum anisotropy are expected to be larger for a CGC based initial condition compared to Glauber model [17]. Hence for other similar conditions in the simulations, the calculations with CGC based initial condition is expected to give higher values of v_2 compared to initialization based on a Glauber model. Earlier comparisons of viscous hydrodynamic simulations with both CGC and Glauber initial conditions to the experimental data at RHIC can be found in Refs [17, 18, 21, 22]. In Ref [17, 18], the experimental data used for comparison are the centrality dependence of multiplicity, $\langle p_T \rangle$, p_T integrated v_2 , and minimum bias v_2 vs. p_T for charged hadrons in Au-Au collisions at $\sqrt{s_{NN}} = 200$ GeV. In general it was observed that calculations with CGC based initial condition prefers a higher value of η/s compared to calculations with a Glauber based initial condition. In Ref [21, 22] the authors have tried to explain the centrality dependence of v_2 divided by the eccentricity with a viscous hydrodynamic model

for the QGP phase coupled to a transport model for the hadronic phase. Comparison of the experimental data to the calculations done for CGC initial condition supports a η/s value $\sim 0.16 - 0.24$. While the corresponding comparisons for a Glauber model based initial condition supports a lower value of $\eta/s \sim 0.08 - 0.16$.

In the current work we compare the results from the viscous hydrodynamics simulations with two different initial conditions (Glauber and CGC) to recent high statistics measurements of $v_2(p_T)$ and $v_4(p_T)$ of charged hadrons in Au-Au collisions at $\sqrt{s_{NN}} = 200$ GeV for a broad range in collision centrality (from 0-10% to 40-50%) [19]. We also compare the simulated results to the measured charged particle invariant yields as a function of p_T for various collision centralities [20].

The paper is organized as follows. In the next section we discuss the formalism of viscous hydrodynamic model used in this work. This includes a brief discussion on the energy-momentum conservation and relaxation equations for shear stress. We present a detailed discussion on the initial conditions used in the calculations. The equation of state used and the freeze-out conditions are also presented. In section III we present a comparative study between calculations with Glauber and CGC initial conditions of various observables in the simulation. These includes the temporal evolution of shear stress, average transverse velocity, and eccentricity. Section IV presents the comparison of viscous hydrodynamic simulations with different input values of η/s for both Glauber and CGC based initial conditions to the experimental data on invariant yield versus p_T , $v_2(p_T)$, and $v_4(p_T)$ for various collision centralities. Finally in section V we present a summary of the work.

II. VISCOUS HYDRODYNAMIC SIMULATION

In a relativistic viscous hydrodynamics scenario, there are two-fold corrections to the ideal fluid hydrodynamics. In presence of the dissipative processes, the energy momentum tensor contains additional dissipative corrections. The equilibrium freezeout distribution function used in the Cooper-Frey freezeout prescription [23] also gets modified. The first order dissipative correction to the energy-momentum tensor leads to acausal behavior [24]. The second order causal viscous hydrodynamics due to Israel-Stewart is one of the most commonly used theory [25]. For the simulation results presented here, we will follow the Israel-Stewart formalism for the evolution of a viscous fluid using the 2+1D viscous hydrodynamic code “AZHYDRO-

KOLKATA” [26, 27]. Shear viscosity is the only dissipative process considered in our present study. We assume a net-baryon free plasma is formed in Au-Au collisions at midrapidity at $\sqrt{s_{NN}} = 200$ GeV.

A. Conservation and relaxation equations

The energy-momentum conservation equation and relaxation equation for shear viscosity in Israel-Stewart formalism is expressed as

$$\partial_\mu T^{\mu\nu} = 0, \quad (1)$$

$$D\pi^{\mu\nu} = -\frac{1}{\tau_\pi}(\pi^{\mu\nu} - 2\eta\nabla^{<\mu}u^{\nu>}) - [u^\mu\pi^{\nu\lambda} + u^\nu\pi^{\mu\lambda}]Du_\lambda. \quad (2)$$

Equation 1 is the conservation equation for the energy-momentum tensor, $T^{\mu\nu} = (\varepsilon + p)u^\mu u^\nu - pg^{\mu\nu} + \pi^{\mu\nu}$. ε , p , and u are the energy density, pressure, and fluid velocity respectively. $\pi^{\mu\nu}$ is the shear stress tensor. Equation 2 is the relaxation equation for the $\pi^{\mu\nu}$. $D = u^\mu\partial_\mu$ is the convective time derivative, $\nabla^{<\mu}u^{\nu>} = \frac{1}{2}(\nabla^\mu u^\nu + \nabla^\nu u^\mu) - \frac{1}{3}(\partial_\mu u^\mu)(g^{\mu\nu} - u^\mu u^\nu)$ is a symmetric traceless tensor. η is the shear viscosity and τ_π is the corresponding relaxation time. Assuming longitudinal boost-invariance, the above equations are solved with the code ‘AZHYDRO-KOLKATA’ in $(\tau = \sqrt{t^2 - z^2}, x, y, \eta_s = \frac{1}{2}\ln\frac{t+z}{t-z})$ coordinates. Where τ is the longitudinal proper time, (t, x, y, z) are space-time coordinates, and η_s is the space time rapidity.

B. Initial conditions

The initial conditions used here includes the initial energy density profile in the transverse plane ($\epsilon(x, y)$), the initial time (τ_i), the transverse velocity profile ($v_x(x, y), v_y(x, y)$), shear stresses in the transverse plane ($\pi^{\mu\nu}(x, y)$) at τ_i . The τ_i value is taken as 0.6 fm. The η/s values are also inputs to the viscous hydrodynamics simulations. We have taken the following temperature independent values for this work, $\eta/s = 0, 0.08, 0.12, 0.16$, and 0.18.

We have considered two different models for the calculation of initial energy density profile in the transverse plane. One is based on a two component Glauber model. At an impact parameter \mathbf{b} , the transverse energy density is obtained from the following two component form

$$\epsilon(\mathbf{b}, x, y) = \epsilon_0[(1-x_h)\frac{N_{part}}{2}(\mathbf{b}, x, y) + x_h N_{coll}(\mathbf{b}, x, y)] \quad (3)$$

where $N_{part}(\mathbf{b}, x, y)$ and $N_{coll}(\mathbf{b}, x, y)$ are the transverse profile of participant numbers and binary collision numbers respectively. ϵ_0 corresponds to the central energy density in $b = 0$ and does not depend on the impact parameter of the collision. The parameter x_h is the hard scattering fraction. Both ϵ_0 and x_h are fixed to reproduce the experimental charged hadron multiplicity density at midrapidity. The $N_{part}(\mathbf{b}, x, y)$ and $N_{coll}(\mathbf{b}, x, y)$ values are obtained using an optical Glauber model calculation [28]. The value of x_h is found to be 0.9 and the values of ϵ_0 for various input values of η/s are given in the Table I.

TABLE I. Values of ϵ_0 used in Glauber model and normalization constant C used in CGC model for initial transverse energy density.

η/s	ϵ_0 (GeV/fm ³), Glauber	C (GeV/fm ^{1/3}) CGC
0.0	43.4	0.11
0.08	36.5	0.095
0.12	32.5	0.085
0.16	27.7	0.070
0.18	25.4	0.065

$$\frac{dN_g}{d^2\mathbf{x}_T dY} = \mathcal{N} \int \frac{d^2\mathbf{p}_T}{p_T^2} \int_{x_1}^{x_2} d^2\mathbf{k}_T \alpha_s(k_T) \phi_A(x_1, (\mathbf{p}_T + \mathbf{k}_T)^2/4; \mathbf{x}_T) \phi_A(x_2, (\mathbf{p}_T - \mathbf{k}_T)^2/4; \mathbf{x}_T), \quad (5)$$

where \mathbf{p}_T and Y are the transverse momentum and rapidity of the produced gluons, respectively. $x_{1,2} = p_T \times \exp(\pm Y)/\sqrt{s}$ is the momentum fraction of the colliding gluon ladders with \sqrt{s} the center of mass collision energy and $\alpha_s(k_T)$ is the strong coupling constant at momentum scale $k_T \equiv |\mathbf{k}_T|$. \mathcal{N} is the normalization constant. The unintegrated gluon distribution functions are taken as

$$\phi(x, k_T^2; \mathbf{x}_T) = \frac{1}{\alpha_s(Q_s^2) \max(Q_s^2, k_T^2)} P(\mathbf{x}_T) (1-x)^4, \quad (6)$$

$P(\mathbf{x}_T)$ is the probability of finding at least one nucleon at transverse position \mathbf{x}_T and is defined as $P(\mathbf{x}_T) = 1 - (1 - \frac{\sigma T_A}{A})^A$, where T_A is the thickness function and σ is the nucleon-nucleon cross section taken as 42 mb. The saturation scale at a given momentum fraction x and transverse coordinate \mathbf{x}_T is given by $Q_s^2(x, \mathbf{x}_T) = 2 \text{ GeV}^2 \left(\frac{T_A(\mathbf{x}_T)/P(\mathbf{x}_T)}{1.53/\text{fm}^2} \right) \left(\frac{0.01}{x} \right)^\lambda$. The growth speed is taken to be $\lambda = 0.28$.

Shear stresses $\pi^{\mu\nu}$ is initialized to their corresponding Navier-Stokes estimates for the boost invariance velocity profile, $\pi^{xx} = \pi^{yy} = 2\eta/3\tau_i$, $\pi^{xy} = 0$ [34]. We have used $\tau_\pi = 3\eta/4p$ (where η and p

The other model commonly used to obtain initial conditions for hydrodynamics is the Color-Glass-Condensate (CGC) approach, based on the ideas of gluon saturation at high energies [29, 30]. We have used the KLN (Kharzeev-Levin-Nardi) k_T -factorization approach [31], due to Drescher *et al.* [32].

We follow references [17, 33] and consider that the initial energy density can be obtained from the gluon number density through the thermodynamic relation,

$$\epsilon(\tau_i, \mathbf{x}_T, b) = C \times \left[\frac{dN_g}{d^2\mathbf{x}_T dY}(\mathbf{x}_T, b) \right]^{4/3}, \quad (4)$$

where $\frac{dN_g}{d^2\mathbf{x}_T dY}$ is the gluon number density evaluated at central rapidity $Y = 0$ and the overall normalization C is a free parameter. C is fixed to reproduce the experimentally measured charged particle multiplicity density at midrapidity. The values of C used in the simulations for different input values of η/s are given in Table I. The number density of gluons produced in a collision of two nuclei with mass number A is given by

are the shear viscous coefficient and pressure) in our simulation, which corresponds to the kinetic theory estimates of relaxation time for shear viscous stress for a relativistic Boltzmann gas [25]. The initial values of $v_x(x, y)$ and $v_y(x, y)$ are taken to be zero.

C. Equation of state

In the present simulations we have used an equation of state with cross-over transition at temperature $T_c = 175$ MeV [35]. The low temperature phase of the EoS is modeled by hadronic resonance gas, containing all the resonances with $M_{res} \leq 2.5$ GeV. The high temperature phase is a parametrization of the recent lattice QCD calculation [36]. Entropy density of the two phases are joined at $T = T_c = 175$ MeV by a smooth step like function. The thermodynamic variables pressure (p), energy density (ϵ), entropy density (s) etc. are then calculated by using the standard thermodynamic relations

$$p(T) = \int_0^T s(T') dT' \quad (7)$$

$$\epsilon(T) = Ts(T) - p(T). \quad (8)$$

D. Freeze-out condition

The hydrodynamic expansion of the hot and dense matter leads to cooling of the system. After some time the mean-free path of the constituent becomes large/comparable to the system size. The system can no longer maintain the local thermal equilibrium and the momentum distribution of the particles remains unchanged after that. This is called freezeout. We use the Cooper-Frey algorithm at the freezeout to calculate invariant yields of the hadrons [23]. The freezeout temperature which is a free parameter in the hydrodynamics simulation is taken as $T_f=130$ MeV. The effect of different choices of freeze-out temperature on charged hadron p_T spectra and elliptic flow is discussed in appendix A.

As we have already pointed out there are twofold correction to the ideal fluid in the presence of viscous effects. The freezeout distribution function for a system slightly away from local thermal equilibrium can be approximated as [26]

$$f_{neq}(x, p) = f_{eq}(x, p)[1 + \phi(x, p)], \quad (9)$$

where $\phi(x, p) \ll 1$ is the corresponding deviation from the equilibrium distribution function $f_{eq}(x, p)$. The non-equilibrium correction $\phi(x, p)$ can be approximated in Grad's 14 moment method by a quadratic function of the four momentum p^μ in the following way [37, 38]

$$\phi(x, p) = \varepsilon - \varepsilon_\mu p^\mu + \varepsilon_{\mu\nu} p^\mu p^\nu, \quad (10)$$

where ε , ε_μ , and $\varepsilon_{\mu\nu}$ are functions of p^μ , metric tensor $g^{\mu\nu}$, and thermodynamic variables.

For our study where only shear stresses are considered, $\phi(x, p)$ has the following form

$$\phi(x, p) = \varepsilon_{\mu\nu} p^\mu p^\nu, \quad (11)$$

where

$$\varepsilon_{\mu\nu} = \frac{1}{2(\epsilon + p)T^2} \pi_{\mu\nu}. \quad (12)$$

As expected, the correction factor increases with increasing values of shear stress $\pi_{\mu\nu}$ at freezeout. The correction term also depends on the particle momentum. The Cooper-Frey formula [23] for a non equilibrium system is

$$\frac{dN}{d^2p_T dy} = \frac{g}{(2\pi)^3} \int d\Sigma_\mu p^\mu f_{neq}(p^\mu u_\mu, T),$$

where g is the degeneracy of the particle considered and $d\Sigma_\mu$ is the normal to the elemental freeze-out hypersurface.

III. GLAUBER VERSUS CGC INITIAL CONDITION

A. Space-time evolution

Figure 1 shows the constant temperature contours corresponding to $T_c = 175$ MeV and $T_f = 130$ MeV in the τ - x plane (at $y = 0$) indicating the boundaries for the QGP and hadronic phases respectively. The results are from the viscous hydrodynamic simulations for Au-Au collisions at impact parameter 7.4 fm and $\eta/s = 0.08$. The solid red curves corresponds to initial transverse energy density profile based on CGC model and the dashed black curve corresponds to results based on Glauber model initial conditions. We observe that the lifetime of QGP and hadronic phases are slightly larger for the simulations based on CGC initial conditions compared to Glauber based initial conditions. The spatial extent of the hadronic phase is slightly smaller for the

simulations with CGC initial conditions relative to Glauber based conditions.

B. Temporal evolution of shear stress

In presence of shear viscosity the thermodynamic pressure is modified. The tracelessness of shear stress tensor $\pi^{\mu\nu}$, along with the assumption of longitudinal boost invariance ensures that at the initial time π^{xx} and π^{yy} components of shear viscous stress are positive. Consequently in viscous fluid the effective pressure in the transverse direction is larger compared to the ideal fluid, for the same thermodynamic condition. It is then important to have some idea how various components of shear viscous stress $\pi^{\mu\nu}$ evolves in space-time. We have considered π^{xx} , π^{yy} , and π^{xy} as the three independent components of shear stress $\pi^{\mu\nu}$. This choice is not unique.

The temporal evolution of spatially averaged π^{xx} , π^{yy} , and π^{xy} are shown in Fig. 2 for CGC (solid red curve) and Glauber (black dashed curve) initialization of energy density. All the three components of $\pi^{\mu\nu}$ becomes zero after time ~ 7 fm irrespective of the CGC or Glauber model initialization. At initial

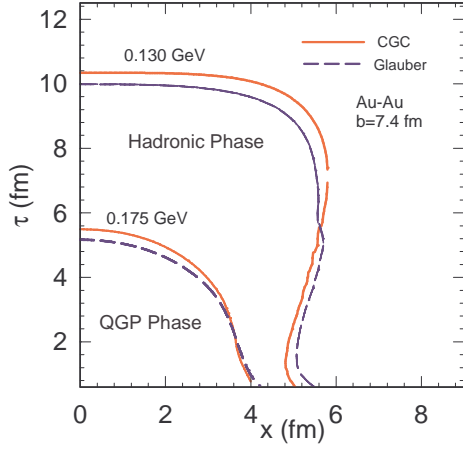


FIG. 1. (Color online) Constant temperature contours denoting the space time boundaries of the QGP and hadronic phases from a 2+1D viscous hydrodynamic simulation with $\eta/s = 0.08$ for Au-Au collisions at impact parameter 7.4 fm. The quark-hadron transition temperature in the simulation is around 175 MeV and freeze-out temperature is taken as 130 MeV. The solid red curves are simulations with initial transverse energy density profile based on CGC model while the dashed black curves correspond to initial conditions based on Glauber model.

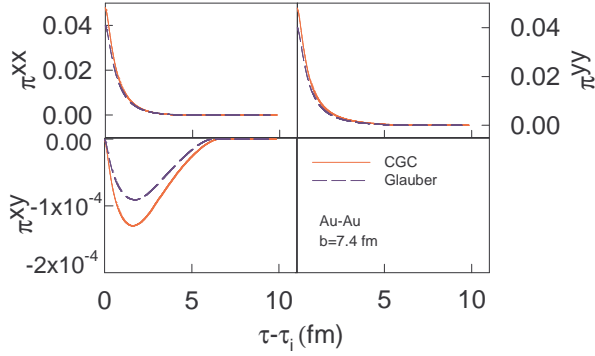


FIG. 2. (Color online) The spatially averaged shear viscous stresses π^{xx} , π^{yy} , and π^{xy} as a function of evolution time for Au-Au collisions at impact parameter 7.4 fm and $\eta/s = 0.08$. The solid red and black dashed curves corresponds to simulations with CGC and Glauber based initial conditions respectively.

time the values of spatially averaged π^{xx} and π^{yy} are observed to be larger for CGC compared to the Glauber initialization. However, the difference vanishes quickly ~ 3 fm. For π^{xy} a noticeable difference is seen for CGC and Glauber model initialization within time ~ 6 fm.

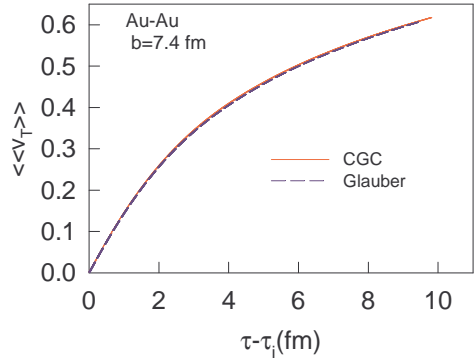


FIG. 3. (Color online) Time evolution of spatially averaged transverse velocity $\langle\langle v_T \rangle\rangle$. The results are from a 2+1D viscous hydrodynamic simulation with $\eta/s = 0.08$. The solid red curve corresponds to simulated result with CGC based initial transverse energy density profile. The black dashed line is the simulated result with Glauber based initial conditions.

C. Average transverse velocity and Eccentricity

Figure 3 shows the temporal evolution of the spatially averaged transverse velocity ($\langle\langle v_T \rangle\rangle$) of the fluid with Glauber based and CGC based initial transverse energy density profile with viscous hydrodynamic simulations carried out for $\eta/s = 0.08$. The simulation is done for Au-Au collisions at impact parameter, $b = 7.4$ fm. The space averaged transverse velocity is defined as $\langle\langle v_T \rangle\rangle = \frac{\langle\langle \gamma \sqrt{v_x^2 + v_y^2} \rangle\rangle}{\langle\langle \gamma \rangle\rangle}$, where $\gamma = \frac{1}{\sqrt{1 - v_x^2 - v_y^2}}$. The angular bracket $\langle\langle \dots \rangle\rangle$ implies an energy density weighted average. Solid red curve is for CGC based initial condition and the dashed black curve is for the Glauber based initial condition. We observe almost no change in the $\langle\langle v_T \rangle\rangle$ as a function of time for the two initial conditions studied. This effect should be reflected in the slope of the invariant yield of the charged hadrons as a function of transverse momentum being same for both the initial conditions. These results are discussed in section IV A.

Figure 4 shows the temporal evolution of the spatial eccentricity (ε_x) and the momentum space anisotropy (ε_p) of the viscous fluid ($\eta/s = 0.08$) with Glauber and CGC based initial conditions for Au-Au collisions at impact parameter, $b = 7.4$ fm. The ε_x which is a measure of the spatial deformation of the fireball from spherical shape is defined as

$$\varepsilon_x = \frac{\langle\langle y^2 - x^2 \rangle\rangle}{\langle\langle y^2 + x^2 \rangle\rangle}, \quad (13)$$

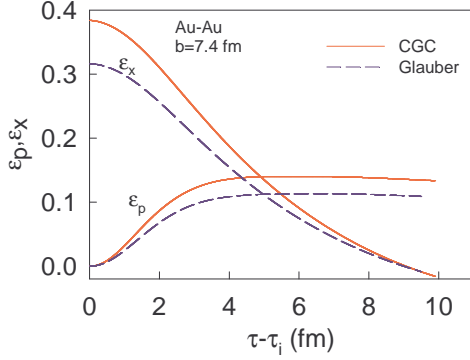


FIG. 4. (Color online) The temporal evolution of spatial (ε_x) and momentum (ε_p) eccentricity for Au-Au collisions at $b=7.4$ fm. The solid red curves corresponds to viscous hydrodynamics ($\eta/s = 0.08$) simulated results with CGC based initial condition and the black dashed lines corresponds to results with Glauber based initial condition.

and the ε_p which is a measure of the asymmetry of fireball in momentum space is defined as

$$\varepsilon_p = \frac{\int dx dy (T^{xx} - T^{yy})}{\int dx dy (T^{xx} + T^{yy})}, \quad (14)$$

where T^{xx} and T^{yy} are the components of energy-momentum tensor $T^{\mu\nu}$. Solid red curve is for CGC based initial condition and the dashed black curve is for the Glauber based initial condition. We find both ε_x and ε_p are higher for the simulated results with CGC based initial condition compared to initial condition based on Glauber model. As the simulated elliptic flow v_2 in hydrodynamic model is directly related to the temporal evolution of the momentum anisotropy, we expect the v_2 for the CGC based initial condition to be larger than the corresponding values for the Glauber based initial condition. These results are discussed in section IV B.

IV. COMPARISON TO EXPERIMENTAL DATA

The experimental data used for comparison to our simulated results are from the PHENIX collaboration at RHIC [19, 20]. The observables used are invariant yield of charged hadrons, elliptic flow, and hexadecapole flow as a function of p_T for Au-Au collisions at pseudorapidity $|\eta| < 0.35$ for $\sqrt{s_{NN}} = 200$ GeV. The high statistics recent PHENIX measurement of elliptic ($k = 1$) and hexadecapole ($k = 2$) flow [19] are obtained using the formula $v_{2k} = \langle \cos(2k(\phi - \Psi_2)) \rangle$ after correction of the event plane resolution. Where ϕ is the azimuthal angle of the charged hadrons and Ψ_2 is the second order

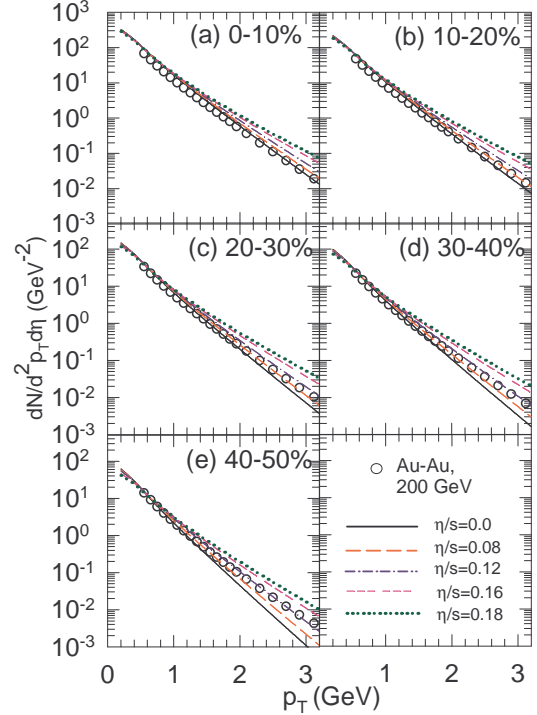


FIG. 5. (Color online) Invariant yield of charged hadrons as a function of transverse momentum at midrapidity for Au-Au collisions at $\sqrt{s_{NN}} = 200$ GeV. The open circles corresponds to experimental data measured by the PHENIX collaboration [20]. The lines represent results from a 2+1D relativistic viscous hydrodynamic model with a Glauber based initial transverse energy density profile and different η/s values. The results are shown for five different collision centralities 0-10%, 10-20%, 20-30%, 30-40%, and 40-50%.

event plane constructed using event plane detectors in $1.0 < |\eta| < 3.9$. The rapidity gap between the detectors used to measure the v_{2k} and Ψ_2 ensures absence of significant $\Delta\eta$ dependent non-flow correlations, which are also absent in our hydrodynamic simulations. Ψ_2 for our simulation is along x axis. We compare below our simulated results on invariant yield, elliptic, and hexadecapole flow for five different collision centralities with input η/s varying between 0.0 to 0.18 to the corresponding experimental data.

A. Invariant yield

Figure 5 shows invariant yield of charged hadrons as a function of transverse momentum at midrapidity for Au-Au collisions at $\sqrt{s_{NN}} = 200$ GeV for five different collision centralities (0-10%, 10-20%, 20-30%, 30-40%, and 40-50%). The open circles are the experimental data from the PHENIX col-

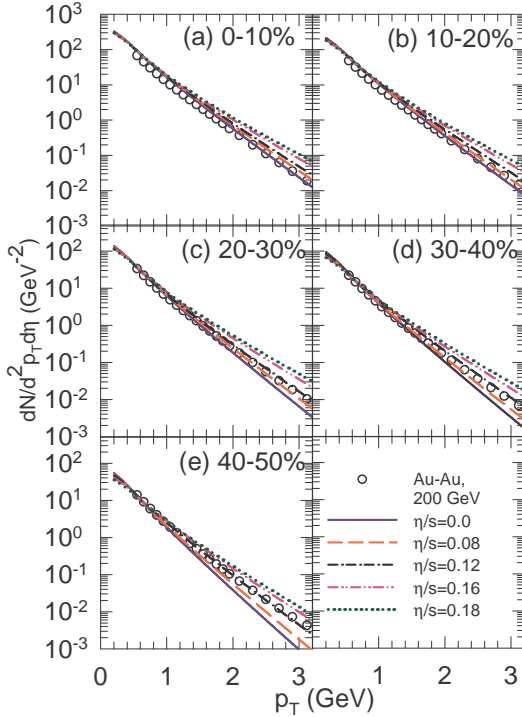


FIG. 6. (Color online) Same as Fig. 5 but the 2+1D relativistic viscous hydrodynamic simulations are done with a CGC based initial transverse energy density profile.

laboration [20]. The simulated results are from the 2+1D relativistic viscous hydrodynamic model with a Glauber based initial transverse energy density profile. The black solid, orange long dashed, purple dash-dotted, magenta short dashed and green dotted lines corresponds to calculations with $\eta/s = 0.0, 0.08, 0.12, 0.16$, and 0.18 respectively. We find the 0-10% experimental data is best explained by simulation with $\eta/s = 0.0$. Whereas data for collision centralities between 20-30% to 40-50% supports a η/s value within 0.08 to 0.12.

Figure 6 shows the same results as in Fig. 5 but the simulated results corresponds to 2+1D viscous hydrodynamic calculations with a CGC based initial transverse energy density profile. The conclusions regarding the comparison between simulated results and experimental data are similar to that obtained for Fig. 5. This also means that the invariant yield of charged hadrons are not very sensitive to the choice of a Glauber based or CGC based initial conditions. The average transverse velocity at the freeze-out which determines the slope of the p_T spectra was observed to be similar for the fluid evolution with Glauber and CGC based initial conditions (see Fig. 3).

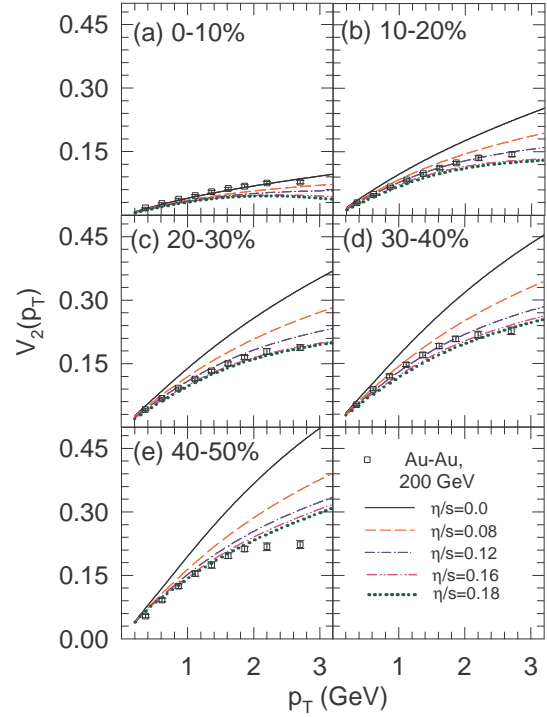


FIG. 7. (Color online) Elliptic flow of charged hadrons as a function of transverse momentum at midrapidity for Au-Au collisions at $\sqrt{s_{NN}} = 200$ GeV. The open circles corresponds to experimental data measured by the PHENIX collaboration [19]. The lines represent results from a 2+1D relativistic viscous hydrodynamic model with a Glauber based initial transverse energy density profile and different η/s values.

B. Elliptic flow

Figure 7 shows the elliptic flow (v_2) as a function of transverse momentum (p_T) for charged hadrons at midrapidity in Au-Au collisions at $\sqrt{s_{NN}} = 200$ GeV. The results are shown for five different collision centralities (0-10%, 10-20%, 20-30%, 30-40%, and 40-50%). The open circles are the experimental data from the PHENIX collaboration [19]. The simulated results are from the 2+1D relativistic viscous hydrodynamic model with a Glauber based initial transverse energy density profile. The black solid, orange long dashed, purple dash-dotted, magenta short dashed, and green dotted lines corresponds to calculations with $\eta/s = 0.0, 0.08, 0.12, 0.16$, and 0.18 respectively. We find the experimental data prefers higher values of η/s as we go from central to peripheral collisions. While 0-10% collision centrality experimental data is best described by ideal fluid ($\eta/s = 0.0$) simulation results, those corresponding to 40-50% collision centrality is closest to simulated results with $\eta/s = 0.18$.

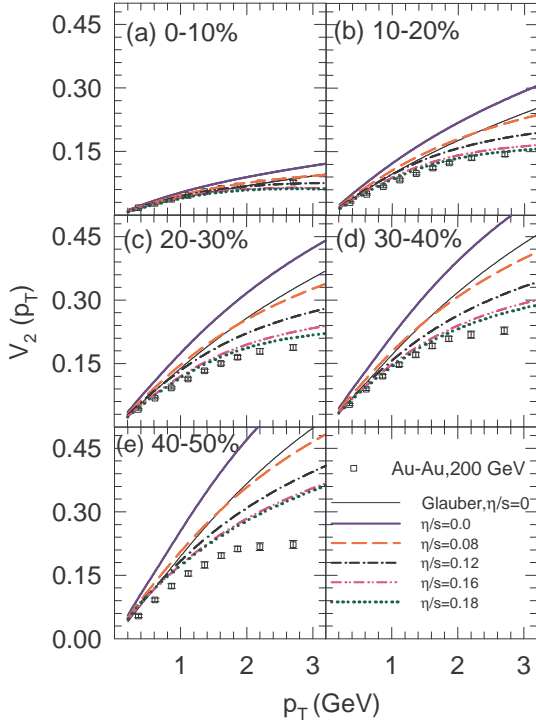


FIG. 8. (Color online) Same as Fig. 7 but the 2+1D relativistic viscous hydrodynamic simulations are done with a CGC based initial transverse energy density profile. Also shown for comparison is the result with Glauber based initial conditions for ideal fluid evolution.

Figure 8 shows the same results as in Fig. 7 but the simulated results corresponds to 2+1D viscous hydrodynamic calculations with a CGC based initial transverse energy density profile. Also shown for comparison the simulated results for ideal fluid evolution with Glauber based initial conditions. We find the $v_2(p_T)$ for CGC based initial condition is larger compared to corresponding results from Glauber based initial conditions. This can be understood from the fact that CGC based initial condition leads to a higher value of momentum anisotropy compared to Glauber based initial condition (as seen in Fig. 4). The general conclusion that the experimental data prefers a higher value of η/s as we go from central to peripheral collisions as seen for viscous hydrodynamic simulations with Glauber based initial conditions also holds for those with the CGC based initial conditions. However, we find from the comparison of experimental data to simulations based on CGC initial conditions that the $v_2(p_T)$ data for 0-10% collisions is best explained for simulated results with η/s between 0.08-0.12. This is in contrast to what we saw from the comparisons of data to simulations with Glauber based initial conditions, where the data preferred $\eta/s = 0.0$ (see Fig. 7). For more

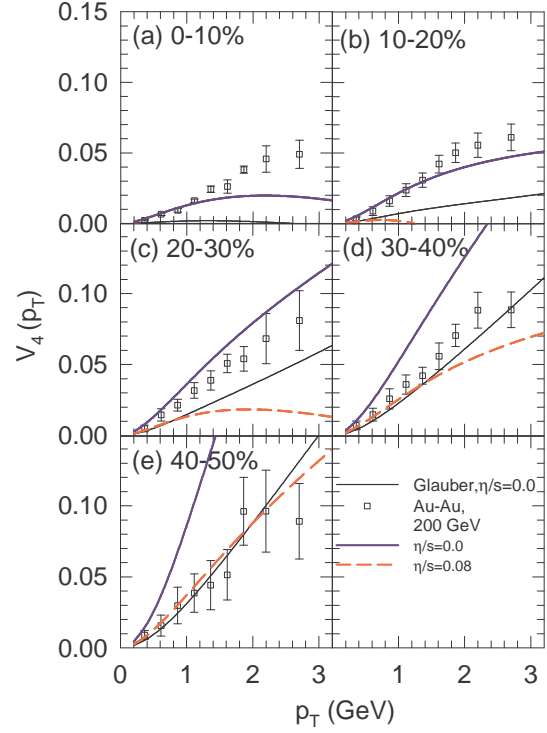


FIG. 9. (Color online) Hexadecapole flow of charged hadrons as a function of transverse momentum at midrapidity for Au-Au collisions at $\sqrt{s_{NN}} = 200$ GeV. The open circles corresponds to experimental data measured by the PHENIX collaboration [19]. The curves represent results from a 2+1D relativistic viscous hydrodynamic model with both Glauber based and CGC based initial transverse energy density profile and different η/s values.

peripheral collisions (centralities beyond 20-30%), it seems data would prefer a higher value of $\eta/s \sim 0.18$. We do not present simulation results for $\eta/s > 0.18$ as the viscous hydrodynamic simulated spectra distributions show a large deviations from ideal fluid simulation results (see appendix B). This leads to a breakdown of the simulation frame work which is designed to be valid for case of small deviations of observables from ideal fluid simulations.

C. Hexadecapole flow

Figure 9 shows the hexadecapole flow (v_4) as a function of transverse momentum (p_T) for charged hadrons at midrapidity in Au-Au collisions at $\sqrt{s_{NN}} = 200$ GeV. The results are shown for five different collision centralities (0-10%, 10-20%, 20-30%, 30-40%, and 40-50%). The open circles are the experimental data from the PHENIX collaboration [19]. Simulated results for only ideal fluid evolution using Glauber based initial condition are shown (solid

black curve). While for the CGC based initial conditions the simulated results are shown for $\eta/s = 0.0$ (purple solid thick curve) and 0.08 (orange dashed curve). We do not present simulated v_4 results for other η/s values as these are much lower compared to the data. We find that $v_4(p_T)$ from ideal hydrodynamic simulations with Glauber based initial conditions under predict the experimental data for all collision centralities studied except for the most peripheral collisions (40-50%) presented. This is in sharp contrast to the observation for $v_2(p_T)$ (see Fig. 7) under similar conditions. Comparison between simulated results with CGC based initial condition and experimental data shows that the preferred η/s lies between 0.0 and 0.08 for the collision centralities studied. The η/s values supported by the data on v_2 and v_4 using the simulated results presented here appears to be different. In this study we have used smooth initial conditions, a more realistic approach is to use a fluctuating initial condition and carry out event-by-event hydrodynamics. This will enable us to study the odd flow harmonics v_3 along with the even harmonics v_2 and v_4 . The simultaneous description of all these experimentally measured flow harmonics in a viscous hydrodynamics framework will probably provide a better estimation of η/s .

V. SUMMARY

We have carried out a 2+1D relativistic viscous hydrodynamic simulation with two different initial conditions (Glauber and CGC) for the transverse energy density profile in Au-Au collisions at $\sqrt{s_{NN}} = 200$ GeV. The simulations are carried out for η/s values between 0.0 to 0.18, using a lattice + hadron resonance gas model based equation of state which has a cross over temperature for the quark-hadron transition at 175 MeV. The shear viscous corrections are considered both in the evolution equations and freeze-out distribution function.

We find that the temporal dependence of the average transverse velocity of the viscous fluid is similar for both the initial conditions studied. The components of shear viscous stress are observed to have higher values for the simulations with CGC initial conditions compared to those for Glauber model initialization at early times of fluid evolution (< 6 fm). The simulated invariant yield of charged particles as a function of transverse momentum is also found to be similar for the Glauber and CGC based initial conditions. The spatial eccentricity and the momentum anisotropy have larger values for simulations with CGC based initial condition compared to the corresponding values for Glauber based initial condition. The simulated elliptic flow is observed to be higher for calculations with CGC based initial con-

ditions relative to those with Glauber based initial conditions, for a given collision centrality.

We have compared our simulated results to the experimental data at midrapidity on the centrality dependence of invariant yield, v_2 , and v_4 as a function of p_T of charged hadrons measured in Au-Au collisions at $\sqrt{s_{NN}} = 200$ GeV. From the comparison to the p_T spectra of charged particles we observe that the data supports a η/s value between 0 to 0.12 for the 0-10% to 40-50% collision centralities for both the initial conditions considered. The $v_2(p_T)$ experimental data requires a lower value of η/s for simulations with Glauber model initialization compared to the CGC based initial conditions. For both the models of initial conditions the $v_2(p_T)$ data indicates a centrality dependence in the estimated η/s value, with peripheral collisions preferring larger values. The experimental data on $v_4(p_T)$ for the collision centralities 0-10% to 40-50% supports a η/s value between 0 - 0.08 for a CGC based initial condition. While simulated results using the Glauber based initial condition for the ideal fluid evolution under estimates the $v_4(p_T)$ for collision centralities 0-10% to 30-40%. Simulations with Glauber model initial conditions explain the $v_4(p_T)$ data for 40-50% collisions with $\eta/s = 0.0$. The observation associated with v_4 is different from v_2 , with v_4 data preferring smaller values of η/s .

There are further scopes of improvement on the simulated results presented here. Recent experimental measurements of odd and higher order azimuthal anisotropic flow [39–41] suggests that a fluctuating initial condition needs to be considered. It is expected that the input η/s to the hydrodynamic simulations has a temperature dependence in both the QGP and hadronic phases [11]. Although large uncertainties still exist in the QCD computations of η/s for the QGP phase. A more precise estimation of η/s would require the viscous fluid simulations to also consider bulk viscosity and vorticity effects [42]. Both of which are expected to be non-zero for the system formed in high energy heavy-ion collisions and may affect the observables like v_2 . A proper prescription for bulk viscous freeze-out correction is still under debate in literature [27, 43, 44], while implementation of vorticity in viscous hydrodynamic simulations have just started to be investigated. We plan to consider some of these effects in the near future.

Acknowledgments

BM is partially supported by the DAE-BRNS project grant No. 2010/21/15-BRNS/2026.

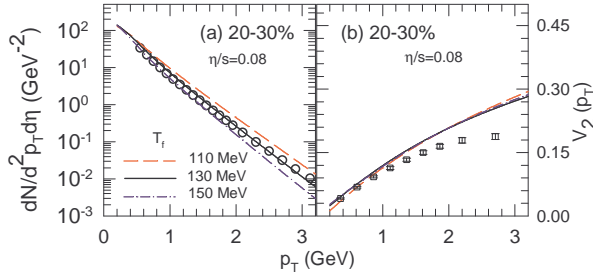


FIG. 10. (Color online) (a) Invariant yield and (b) elliptic flow of charged hadrons as a function of transverse momentum at midrapidity for Au-Au collisions at $\sqrt{s_{NN}} = 200$ GeV. The open circles corresponds to experimental data measured by the PHENIX collaboration [19]. The lines represent results from a 2+1D relativistic viscous hydrodynamic model with a Glauber based initial transverse energy density profile with $\eta/s = 0.08$ and different T_f values.

Appendix A: Freezeout temperature

We have studied the effect of different freeze-out temperature on the charged hadron invariant yield and elliptic flow. Figure 10 shows the invariant yield (panel - a) and elliptic flow (panel - b) of charged hadrons for 20-30% centrality Au-Au collisions at $\sqrt{s_{NN}} = 200$ GeV. All the simulated results are for $\eta/s = 0.08$ using the same Glauber based initial condition but with three different freeze-out temperatures, $T_f = 110$ (red dashed curve), 130 (black solid curve), and 150 MeV (blue dash-dotted curve).

The slope of the p_T spectra increases as T_f decreases. This is because of higher radial velocity gained due to longer duration of evolution of the system for the lower freeze-out temperature. The experimentally measured p_T spectra is best explained for simulations with input parameters as specified in section II and $T_f = 130$ MeV.

For the current simulations the effect of different T_f values studied is observed to be small on elliptic flow of charged hadrons. This could possibly be due to saturation of the value of the momentum anisotropy at the early time of evolution.

Appendix B: Viscous correction

There are two kinds of dissipative correction to the ideal fluid simulation. First the energy momen-

tum tensor contains a viscous correction and the freezeout distribution function is also modified in presence of the dissipative processes. The viscous hydrodynamics model is applicable when the dissipative correction (both in the energy-momentum tensor and freezeout distribution function) is small

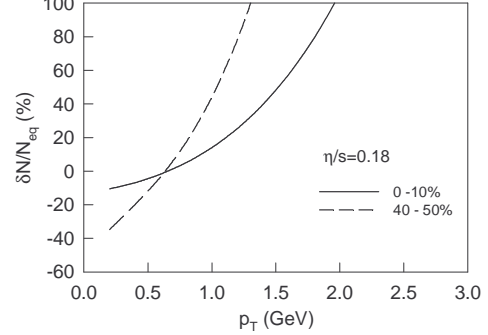


FIG. 11. Dissipative correction to the invariant yield of the charged hadron as a function of p_T for 0-10% (black solid curve) and 40-50% centrality (black dashed curve) Au-Au collisions at $\sqrt{s_{NN}} = 200$ GeV. The results are shown for $\eta/s = 0.18$ and Glauber based initial condition.

compared to the corresponding equilibrium value. It is then implied that the relative viscous correction ($\delta N/N_{eq}$) is small for the Israel-Stewart's hydrodynamics to be applicable, where N_{eq} is the invariant yield for system in local thermal equilibrium, and $\delta N = \frac{dN}{d^2 p_T}|_{viscous} - \frac{dN}{d^2 p_T}|_{equilibrium}$. In figure 11 the relative viscous correction $\delta N/N_{eq}$ for $\eta/s = 0.18$ are shown for 0-10% (black solid curve) and 40-50% (black dashed curve) collision centrality. We observe that the relative shear viscous correction is quite large ($\sim 50\%$) at $p_T \sim 1.0$ GeV for 40-50% centrality (dashed curve in figure 11). The solid curve in the same figure shows the relative viscous correction to the invariant yield of charged hadron for Au-Au collision for 0-10% centrality at $\sqrt{s_{NN}} = 200$ GeV. A higher value of η/s will introduce a larger viscous correction and eventually the viscous hydrodynamics framework will no longer be applicable.

[1] I. Arsene *et al.* [BRAHMS Collaboration], Nucl. Phys. A **757**, 1 (2005).

[2] B. B. Back *et al.*, Nucl. Phys. A **757**, 28 (2005).

- [3] J. Adams *et al.* [STAR Collaboration], Nucl. Phys. A **757**, 102 (2005).
- [4] K. Adcox *et al.* [PHENIX Collaboration], Nucl. Phys. A **757**, 184 (2005).
- [5] M. Gyulassy and L. McLerran, Nucl. Phys. A **750**, 30 (2005).
- [6] J. Xu and C. M. Ko, Phys. Rev. C **84**, 014903 (2011).
- [7] V. Greco, J. Phys. Conf. Ser. **336**, 012017 (2011).
- [8] B. H. Alver, C. Gombeaud, M. Luzum and J. Y. Ollitrault, Phys. Rev. C **82**, 034913 (2010).
- [9] N. Demir and S. A. Bass, Eur. Phys. J. C **62**, 63 (2009).
- [10] R. S. Bhalerao, J. P. Blaizot, N. Borghini and J. Y. Ollitrault, Phys. Lett. B **627**, 49 (2005).
- [11] H. Niemi, G. S. Denicol, P. Huovinen, E. Molnar and D. H. Rischke, Phys. Rev. Lett. **106**, 212302 (2011).
- [12] C. Shen, U. Heinz, P. Huovinen and H. Song, Phys. Rev. C **82**, 054904 (2010).
- [13] U. W. Heinz, J. S. Moreland and H. Song, Phys. Rev. C **80**, 061901 (2009).
- [14] A. K. Chaudhuri, Phys. Lett. B **681**, 418 (2009).
- [15] P. Bozek, Phys. Rev. C **81**, 034909 (2010).
- [16] B. Schenke, S. Jeon and C. Gale, Phys. Rev. Lett. **106**, 042301 (2011).
- [17] M. Luzum and P. Romatschke, Phys. Rev. C **78**, 034915 (2008) [Erratum-ibid. C **79**, 039903 (2009)].
- [18] M. Luzum and P. Romatschke, Phys. Rev. Lett. **103**, 262302 (2009).
- [19] A. Adare *et al.* [PHENIX Collaboration], Phys. Rev. Lett. **105**, 062301 (2010).
- [20] S. S. Adler *et al.* [PHENIX Collaboration], Phys. Rev. C **69**, 034910 (2004).
- [21] H. Song, S. A. Bass, U. Heinz, T. Hirano and C. Shen, Phys. Rev. Lett. **106**, 192301 (2011).
- [22] H. Song, S. A. Bass, U. Heinz, T. Hirano and C. Shen, Phys. Rev. C **83**, 054910 (2011).
- [23] F. Cooper and G. Frye, Phys. Rev. D **10**, 186 (1974).
- [24] W. A. Hiscock and L. Lindblom, Phys. Rev. D **31**, 725 (1985).
- [25] W. Israel and J. M. Stewart, Annals Phys. **118**, 341 (1979) ; Ann. Phys. (N.Y.) **100**, 310 (1976).
- [26] A. K. Chaudhuri, arXiv:0801.3180 [nucl-th].
- [27] V. Roy and A. K. Chaudhuri, Phys. Rev. C **85**, 024909 (2012).
- [28] M. L. Miller, K. Reygers, S. J. Sanders and P. Steinberg, Ann. Rev. Nucl. Part. Sci. **57**, 205 (2007).
- [29] L. D. McLerran and R. Venugopalan, Phys. Rev. D **49**, 3352 (1994).
- [30] L. D. McLerran and R. Venugopalan, Phys. Rev. D **49**, 2233 (1994).
- [31] D. Kharzeev, E. Levin and M. Nardi, Nucl. Phys. A **730** (2004) 448 [Erratum-ibid. A **743** (2004) 329].
- [32] H. J. Drescher, A. Dumitru, A. Hayashigaki and Y. Nara, Phys. Rev. C **74** (2006) 044905.
- [33] A. Dumitru, E. Molnar and Y. Nara, Phys. Rev. C **76**, 024910 (2007).
- [34] A. K. Chaudhuri, Phys. Lett. B **672**, 126 (2009).
- [35] V. Roy and A. K. Chaudhuri, Phys. Lett. B **703**, 313 (2011).
- [36] S. Borsanyi *et al.*, JHEP **1011**, 077 (2010).
- [37] A. Muronga and D. H. Rischke, arXiv:nucl-th/0407114.
- [38] A. Muronga, Phys. Rev. C **76**, 014910 (2007).
- [39] A. Adare *et al.* [PHENIX Collaboration], Phys. Rev. Lett. **107**, 252301 (2011).
- [40] K. Aamodt *et al.* [ALICE Collaboration], Phys. Rev. Lett. **107**, 032301 (2011).
- [41] G. Aad *et al.* [ATLAS Collaboration], arXiv:1203.3087 [hep-ex].
- [42] F. Becattini, F. Piccinini and J. Rizzo, Phys. Rev. C **77**, 024906 (2008).
- [43] A. Monnai and T. Hirano, Phys. Rev. C **80**, 054906 (2009).
- [44] K. Dusling and T. Schafer, Phys. Rev. C **85**, 044909 (2012) [arXiv:1109.5181 [hep-ph]].